# A Linear Regression Model with Dynamic Pulse Transit Time Features for Noninvasive Blood Pressure Prediction

Yi-Yen Hsieh[1], Ching-Da Wu[3] and Shey-Shi Lu[4]
Dept. of Electrical Engineering
National Taiwan University
Taipei, Taiwan
R04943057@ntu.edu.tw

Yu Tsao[2]
Research Center for Information Technology Innovation
Academia Sinica
Taipei, Taiwan
yu.tsao@citi.sinica.edu.tw

***Abstract*— Cardiovascular diseases (CVDs) have become the leading cause of death globally (as reported by the World Health Organization, June 2016). An effective method of preventing CVDs is to measure and monitor blood pressure (BP), which serves as a physiological indicator for cardiovascular systems. A previous research has proposed the use of pulse transit time (PTT) information to compute the BP measure. We propose herein a novel method based on a linear regression model that incorporates static and dynamic PTT features to predict BP measures more accurately. Moreover, the proposed model considers the estimated systolic blood pressure (SBP) when estimating the diastolic blood pressure (DBP). Experimental results first show that the proposed method can predict the BP more accurately than conventional methods, with notably higher correlation scores and lower mean square errors. These results confirm the effectiveness of incorporating dynamic PTT features for accurate BP predictions. Next, our experimental results demonstrate that the proposed method attains a better DBP prediction capability, showing that the estimated SBP provides useful information for the DBP prediction.**

***Keywords—blood pressure; pulse transit time; dynamic feature; blood pressure oscillations***

## I. INTRODUCTION

Blood pressure (BP) is one of the most important physiological indicators for measuring the cardiovascular system (CVS) conditions in the human body. BP measurements can generally be divided into two categories as follows: invasive and non-invasive methods. In the invasive methods, a catheter is inserted into a blood vessel to estimate the BP in a direct manner. This measurement category is precise and reliable. However, it brings additional risks of contamination and uncomfortable feeling to people [1]. In the non-invasive methods, the auscultatory and oscillometric approaches are two popular techniques that have been widely used to clinically estimate the BP. These non-invasive methods are easier and safer compared to their invasive counterparts. However, they have a limited capability of providing real-time measurements and may impose movement restrictions on people during measurement. Some novel non-invasive methods have recently been proposed with technology advancement. Successful examples include arterial tonometry [2, 3] and pulse transit-time (PTT) methods [4–7]. The arterial tonometer method is performed by putting a strain gauge pressure sensor on the radial artery and applying preloading on the sensor to slightly flatten the artery. The arterial pressure is then transmitted from the vessel to the sensor. Although the tonometry methods can continuously predict BP waveforms, unwanted motion artifacts may affect their predication accuracies [8]. Consequently, the subjects are often asked to stay still during measurements when the tonometry methods are used.

The PTT denotes the interval of the arterial blood pressure (ABP) propagation travels from the aortic valve to a peripheral site [4–7]. The PTT has been popularly used in recent years as a feature to predict BP in a non-invasive and real-time manner. The PTT-based methods have a great potential for implementation in portable devices because they can provide a long period of BP monitoring without requiring professional assistances. They are also free from mechanical interferences and provide a feeling of less discomfort. A linear regression (LR) model with a static PTT feature has been derived in previous studies [5–9] to predict the systolic blood pressure (SBP) and the diastolic blood pressure (DBP) as follows:

$$SBP = a_1 * PTT + c_1 \quad (1)$$

$$DBP = a_2 * PTT + c_2 \quad (2)$$

where $a_1$, $a_2$, $c_1$and $c_2$ all are coefficients.

We proposed herein two extensions to the original LR model. First, we proposed the use of the dynamic PTT features for BP predictions. Next, we proposed to incorporate estimated SBP to predict the DBP. The experimental results showed that the proposed method achieved notably higher accuracies of BP predictions than the method that only used static PTT features. The results also revealed that the estimated SBP provides useful information for the DBP predictions.

## II. METHOD

Fig. 1 shows the definition of the PTT feature used in this study. As can be seen in the figure, the PTT feature is estimated from the time period between the R-peak of electrocardiography (ECG) waveforms and the peaks of the first-order derivative of photoplethysmography (PPG) signals,

which correspond to the points with the maximum slope of each PPG signal waveform.

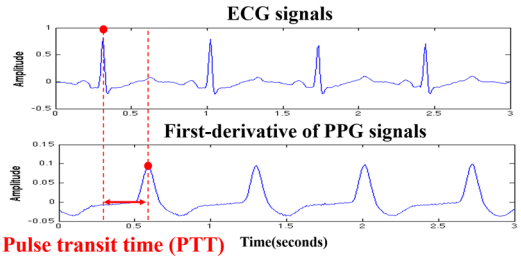


Fig. 1. Definition of the pulse transit time (PTT).

The dynamic PTT features were extracted by (3)-(5) as follows,

$$\Delta PTT_t(j) = \frac{\sum_{m=-q}^{q} m \cdot PTT_{t-m}(j)}{\sum_{m=-q}^{q} m^2} \quad (3)$$

$$\Delta PTT_t{}^2(j) = \frac{\sum_{m=-q}^{q} m \cdot \Delta PTT_{t-m}(j)}{\sum_{m=-q}^{q} m^2} \quad (4)$$

$$\vdots$$

$$\Delta PTT_t{}^K(j) = \frac{\sum_{m=-q}^{q} m \cdot \Delta PTT_{t-m}{}^{K-1}(j)}{\sum_{m=-q}^{q} m^2} \quad (5)$$

where $K$ denotes the $K$-th order dynamic PTT feature, $j$ denotes the sample index, and $q$ determines the size of context window, which determines the context information considered when estimating the dynamic features. In this study, we set $q$=1 for (3)-(5). The dynamic PTT features denote the different-order derivatives of PTT features versus time, representing the dynamic change of the static PTT features. For example, $\Delta PTT_t$ and $\Delta PTT_t{}^2$ refer to the slope and the curvature of static PTT feature, respectively [10]. With the extracted dynamic PTT features, we adopted a feature selection process to filter out the dynamic PTT features that are less correlated to the BP prediction task. Only those features, whose p-values were smaller than 0.0001, were selected to build the LR model. In a preliminary study, we also noted that the DBP synchronously fluctuates with the SBP. Therefore, the values of the estimated SBP were also used as a parameter for the DBP predictions in our model. The proposed model is given by (6) and (7):

$$SBP_{est} = a_1 PTT + \boldsymbol{b}_1^T[\boldsymbol{DPTT}] + c_1 \quad (6)$$

$$DBP_{est} = a_2 PTT + \boldsymbol{b}_2^T[\boldsymbol{DPTT}] + c_2 + d_2 SBP_{est} \quad (7)$$

where $[\boldsymbol{DPTT}] = [\Delta PTT^2, \Delta PTT^4, \Delta PTT^6, \Delta PTT^8, \Delta PTT^{10}]^T$ is the vector of the dynamic PTT features selected by the feature selection process; $a_1$, $c_1$, $a_2$, $c_2$, and $d_2$ are coefficients; and $\boldsymbol{b}_1^T = [f_1, g_1, h_1, i_1, j_1]$, $\boldsymbol{b}_2^T = [f_2, g_2, h_2, i_2, j_2]$ are coefficient vectors. The LR model parameters, including $a_1$, $c_1$, $a_2$, $c_2$, $d_2$, $\boldsymbol{b}_1$, and $\boldsymbol{b}_2$, were estimated based on the minimum square error (MSE) criterion. A comparison of (1) and (2) with (6) and (7), respectively, shows that the proposed model considers additional dynamic features into the LR model. We also included the estimated SBP value when computing the DBP in (7). Fig. 2 shows the overall training and testing phases of the proposed LR model. In the training phase, we estimated the LR model based on (6) and (7) using the training data. The inputs in the testing phase are static and dynamic PTT features. The outputs are the predicted SBP and DBP values. The predication performance is computed based on the correlations and deviations of the predicted SBP/DBP and golden SBP/DBP.

## III. Experiments

In this section, we first test the SBP and DBP prediction performances of the proposed method. We then visually investigate the prediction results of the proposed method with the trajectory plots of the beat-to-beat predicted SBP and DBP values. Finally, we investigate the necessity of re-calibrating the proposed method.

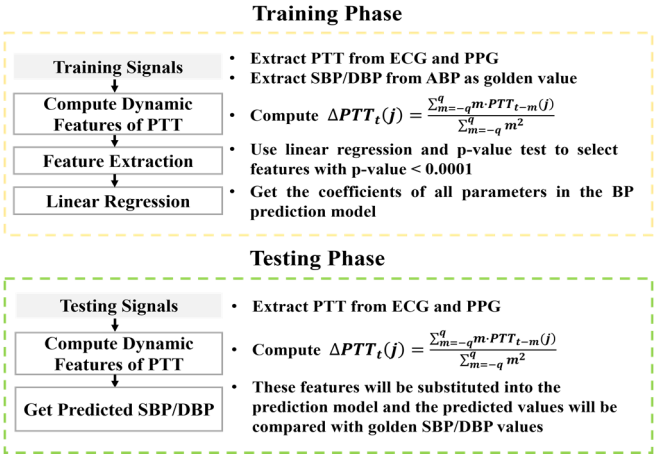


Fig. 2. Flow of the proposed model for the non-invasive BP prediction.

### *3.1 Quantitative SBP and DBP Prediction Results*

Five subjects were selected from the MIMIC database to evaluate the proposed BP prediction algorithm [11]. Fully continuous ECG, PPG, and ABP signals were available for these subjects. One of these subjects has hypertension and an SBP of about 200 mm Hg. The other subjects' systolic BPs ranged between 85 mm Hg and 140 mm Hg. Table I shows the detailed BP records of these five subjects. Each of the ECG, PPG, and ABP signals for each subject was divided into two parts: the training and testing sets. The training set comprising 1-HR continuous beat-to-beat ECG, PPG, and ABP signals was used to estimate the coefficients in the prediction models. The test set was used to evaluate the prediction performance. Golden (ground-truth) SBP and DBP values were extracted from the peaks and valleys of the ABP signals. We evaluated the prediction performances using the correlation of determinations ($R^2$, the correlation of golden BP and the estimated BP) and the mean square error (MSE, point-by-point error measurement). A higher score denotes a better BP prediction result for $R^2$. Meanwhile for MSE, a lower value represents better BP prediction results.

TABLE I. The Five Subjects (from the MIMIC database) in this Study.

| | Target A | Target B | Target C | Target D | Target E |
|---|---|---|---|---|---|
| **Record Number** | 039m | 211m | 212m | 055m | 230m |
| **Type** | Normal | Hypertension | Normal | Normal | Normal |

We compare the SBP and DBP prediction results in Figs. 3 and 4, respectively. In the discussion that follows, the results of the model with only the static PTT feature (i.e., (1) and (2)) and those of the proposed model with both static and dynamic PTT features (i.e., (6) and (7)) are denoted as "LR-S" and "LR-SD", respectively. Tables II and III present the corresponding MSE scores. We conducted an additional test, entitled "LR-SD (no SBP)", for the DBP results in Fig. 4 and Table III to verify the effectiveness of incursion in the estimated SBP value in DBP estimation (7). In that case, the model becomes:

$$DBP_{est} = a_3 PTT + \boldsymbol{b}_3^T[\boldsymbol{DPTT}] + c_3 \qquad (8)$$

We first note from the results of Fig. 3 and Table II that the LR-SD notably outperforms LR-S in terms of the $R^2$ score and the MSE value. This result confirms the effectiveness of using dynamic PTT features into the LR model for SBP prediction. Next, we observe from the results of Fig. 4 and Table III that LR-SD notably outperforms LR-S. This finding again confirms the effectiveness of incorporating the dynamic PTT features into the LR for DBP prediction. Finally, we note from Fig. 4 and Table III that LR-SD clearly outperforms LR-SD (no SBP). This result shows that integrating the estimated SBP value into the LR model can further improve the DBP prediction capability.

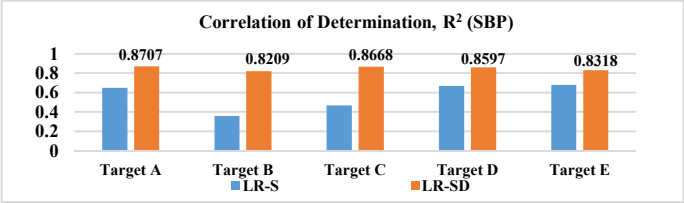


Fig. 3. SBP prediction results in terms of correlations ($R^2$).

TABLE II. SBP PREDICTION RESULTS IN TERMS OF MSE.

| Methods | Target A | Target B | Target C | Target D | Target E |
|---|---|---|---|---|---|
| LR-S | 70.37 | 280.79 | 7.04 | 64.35 | 56.56 |
| LR-SD | **25.85** | **79.51** | **5.13** | **27.4** | **29.54** |

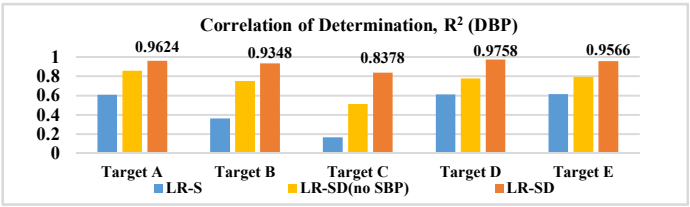


Fig.4. DBP prediction results in terms of correlations ($R^2$).

TABLE III. DBP PREDICTION RESULTS IN TERMS OF MSE

| Methods | Target A | Target B | Target C | Target D | Target E |
|---|---|---|---|---|---|
| LR-S | 30.02 | 19.5 | 5.1 | 38.32 | 25.31 |
| LR-SD(noSBP) | 10.93 | 7.67 | 4.12 | 21.94 | 13.51 |
| LR-SD | **2.88** | **2.02** | **2.24** | **2.39** | **2.86** |

### *3.2 Qualitative SBP/DBP Prediction Results*

In this section, we intend to visually investigate the SBP/DBP prediction results obtained using the proposed method. Figs. 5 and 6 demonstrate the beat-to-beat predicted SBP and DBP of target C, respectively, which include 70 min and 5985 points. The *x*- and *y*-axes in these two figures show the time index and BP values (in mmHg), respectively. The proposed LR-SD in these two figures can generally predict the BP value accurately even though the golden SBP and DBP values drastically change in a very short time period from time to time. According to the Association for the Advancement of Medical Instrumentation criterion, a high-performance BP prediction has the following requirements: 1) the mean of absolute differences between the predicted and golden values must be smaller than 5 mm Hg; 2) the standard deviation of the prediction error must be smaller than 8 mm Hg. The proposed prediction method in Figs. 5 and 6 may not always fit these two requirements after performing prediction in a long time period. Therefore, re-calibration is required. These results are consistent with those reported in the previous studies (e.g., [5][7][9]). We also noted that the re-calibration period for targets with a normal BP (targets A, C, D, E), can be longer (around 80 min). Meanwhile, the re-calibration period is shorter (around 40 min) for a hypertensive subject (Target B).

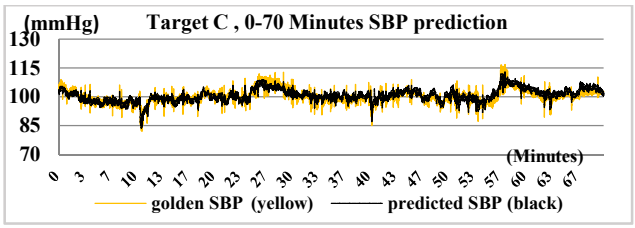


Fig. 5. Target C : 0-70 min of SBP prediction.

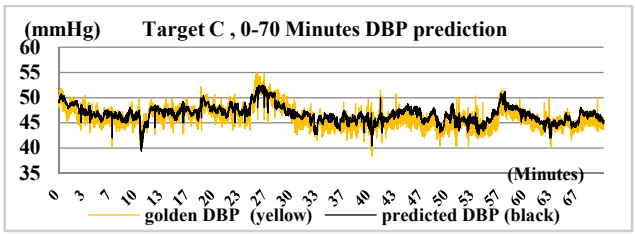


Fig. 6. Target C : 0-70 min of DBP prediction.

### *3.3. Spectral Analyses on the SBP/DBP Prediction Errors*

We present the spectral analysis performed on Target B (the hypertensive individual with the shortest re-calibration period) to investigate the necessity of re-calibration as shown in the previous section. A spectral analysis plot shows the characteristics of a temporal signal in the frequency domain, where the *x*- and *y*-axes denote frequency (Hz) and magnitude, respectively. Figs. 7 and 8 respectively show the 1-hour spectral analysis plots of the golden and predicted SBPs for Target B. Fig. 7 shows three apparent peaks at frequencies around 0.075 Hz, 0.15 Hz, and 0.225 Hz, just similar to the BP rhythmic oscillations that were identified as three components: low frequency (LF, 0.02-0.07 Hz), mid frequency (MF, about 0.1 Hz) and high frequency (HF, 0.2-0.4 Hz) [12]. However, we did not notice such peaks in Fig. 8. For a more in-depth analysis, we estimate the 1-hour spectral prediction errors (= $predicted\ SBP - golden\ SBP$), and show the results in Fig.

9. Fig. 9 illustrates the dotted lines dividing each sub-plot into two parts. The regions belonging to the left part of the dotted lines indicate that the accumulated sum of the squared prediction errors ($=\sum prediction\ error^2$) has reached more than 99.9999%. Figs. 7 to 9 also show that although the predicted SBP in Fig. 8 did not generate the peaks as those noted in the golden SBP, most of the prediction errors are located under BP oscillations at 0.075 Hz (LF).

The abovementioned analyses conclude that the proposed LR-SD model has a limited capability to accurately predict the trend of BP variation at LF. Therefore, a re-calibration is also required, which is consistent with many previous studies using the PTT feature for BP prediction [5][7][9]. Moreover, previous bodies of research have reported that the LF part of BP oscillations often varies as a function of both complex internal and external factors [12]. The internal factors include neurogenic, humoral, and endocrine system factors [13] while the external factors may include temperature [14] and physical activities [15], among others. The deficiency of the proposed model for the BP reaction at LF is likely caused by these internal and external factors.

## IV. CONCLUSION

This paper proposes an LR model for SBP and DBP predictions. The experimental results on five subjects (one with hypertension and four normal people) excerpted from the MIMIC database confirmed that the proposed model achieves better BP prediction results than the conventional ones. The primary contribution of this paper is twofold. First, with the BP oscillations containing complex spectral information on a non-uniform frequency scale [12], we confirm the effectiveness of using both static and dynamic PTT features to attain a better BP prediction capability for both hypertensive and normal people. Second, we confirm the positive effect of incorporating estimated SBP to estimate the DBP. The spectral analysis plots for systolic SBP oscillations revealed that the re-calibration process remains necessary for the proposed model to overcome the deficiencies caused by internal and external factors. In the future, we will expand on our current model by incorporating these factors to further improve the BP prediction capability.

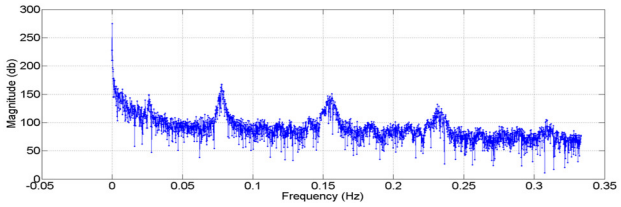


Fig. 7. 1-hour spectral analysis plots of the golden SBP.

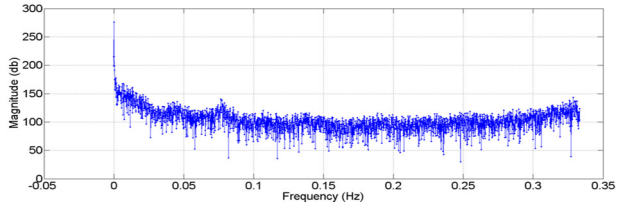


Fig. 8. 1-hour spectral analysis plots of the predicted SBP.

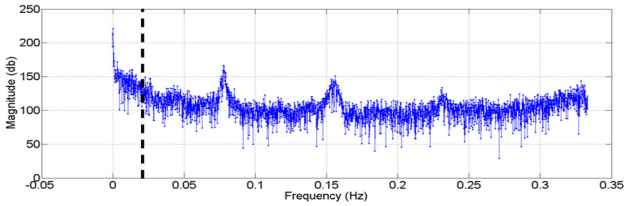


Fig. 9. 1-hour spectral analysis plots of the prediction errors.

## ACKNOWLEDGMENT

The authors gratefully acknowledge National Taiwan University and Ministry of Science and Technology, ROC (MOST 104-2221-E-002-148 MY2) for supporting this research project.

## REFERENCE

[1] H. Sorvoja, "Noninvasive blood pressure pulse detection and blood pressure determination" Kirsti Nurkkala, Ed. Oulu, Finland: Oulu University, 2006, pp. 17–33.

[2] C. Dagdeviren et al., "Conformable amplified lead zirconate titanate sensors with enhanced piezoelectric response for cutaneous pressure monitoring," Nature Commun., vol. 5, August 2014, Num. 4456.

[3] M. R. Nelson, J. Stepanek, M. Cevette, M. Covalciuc, R. T. Hurst, and A.J. Tajik, "Noninvasive measurement of central vascular pressures with arterial tonometry: clinical revival of the pulse pressure waveform?", Mayo Clin. Proc., May 2010, pp.460–472.

[4] C. C. Poon and Y. T. Zhang, ''Cuff-less and noninvasive measurements of arterial blood pressure by pulse transit time,'' Conf. Proc. IEEE Eng. Med. Biol. Soc., vol. 6, 2005, pp. 5877–5880.

[5] A. Jadooei, Zaderykhin O, Shulgin V.I., "Adaptive algorithm for continuous monitoring of blood pressure using a pulse transit time," Proc. IEEE XXXIII Int. Sci. Conf. Electron. Nanotechnol, April 2013, pp. 297–301.

[6] S. Y. Ye, G. R. Kim, D. K. Jung, S.W. Baik, and G.-R. Jeon "Estimation of systolic and diastolic pressure using the pulse transit time," J. World Acad Sci Eng Technol, vol. 43, 2010, pp.726–731.

[7] W. Chen, T. Kobayashi, S. Ichikawa, Y. Takeuchi and T. Togawa, "Continuous estimation of systolic blood pressure using the pulse transit time and intermittent calibration," Med Biol Eng Comput, vol. 38(5), Sept. 2000, pp. 567–574.

[8] E. J. Ciaccio, G. M. Drzewiecki, "Tonometric Arterial Pulse Sensor with Noise Cancellation", IEEE Transactions on Biomedical Engineering, Vol.55, No.10, October 2008. pp. 2388–2396.

[9] F. S. Cattivelli, H. Garudadri, "Noninvasive cuffless estimation of blood pressure from pulse arrival time and heart rate with adaptive calibration," Proc. of Sixth International Workshop on Wearable and Implantable Body Sensor Networks (BSN 2009), 2009, pp. 114–119.

[10] S. Furui, "Cepstral analysis technique for automatic speaker verification," IEEE Trans. Acoustic, Speech, Signal Process., vol. ASSP-29, no. 2, Apr. 1981, pp. 254–272.

[11] G. B. Moody and R. G. Mark, "A database to support development and evaluation of intelligent intensive care monitoring," in Proc. Computers in Cardiology, September 1996, pp.657-660.

[12] G. Parati, J. P. Saul, M. D. Rienzo, and G. Mancia, "Spectral analysis of blood pressure and heart rate variability in evaluating cardiovascular regulation: A critical appraisal," Hypertension, vol. 25, 1995, pp. 1276–1286.

[13] A. Niemirska, M. Litwin, J. Feber, and E. Jurkiewicz "Blood pressure rhythmicity and visceral fat in children with hypertension," Hypertension, vol.62, 2013, pp.782–788.

[14] F. P. Knowlton and E. H. Starling "The influence of variations in temperature and blood-pressure on the performance of the isolated mammalian heart," J Physiol, vol. 44, 1912, pp. 206–219.

[15] O. Tochikubo, A. Ikeda, E. Miyajima, M. Ishii "Effects of insufficient sleep on blood pressure monitored by a new multibiomedical recorder," Hypertension. vol.27, 1996, pp.318–324.